

# Propane and oxygen action on NO<sub>x</sub> adspecies on low-exchanged Cu-ZSM-5

E.V. Rebrov<sup>a</sup>, A.V. Simakov<sup>b,\*</sup>, N.N. Sazonova<sup>b</sup>, V.A. Rogov<sup>b</sup> and G.B. Barannik<sup>b</sup>

<sup>a</sup> Novosibirsk State University, Novosibirsk 630090, Russia

<sup>b</sup> Federal Scientific Center "Boreskov Institute of Catalysis", Novosibirsk 630090, Russia

Received 29 August 1997; accepted 12 January 1998

A surface intermediate with a C/N ratio close to 3 has been shown by TPD to form at co-adsorption of NO and propane as well as NO, propane and O<sub>2</sub> on low-exchanged Cu-ZSM-5. The adsorption of NO, propane and oxygen has been studied to evaluate their effect on the formation of this complex. Its formation is accompanied by a decrease in the concentration of surface nitrite–nitrate. The kinetics of nitrite–nitrate adspecies formation as a function of the reagents concentration and temperature has been investigated. Some NO adspecies have been found to decompose yielding N<sub>2</sub>O.

**Keywords:** NO, adsorption, Cu-ZSM-5, TPD, nitrosopropane, N<sub>2</sub>O

## 1. Introduction

The selective catalytic reduction (SCR) is the most encouraging way to remove NO<sub>x</sub> from industrial gases. Peculiarities of this reaction were extensively investigated on various catalytic systems [1,2]. Cu-ZSM-5 catalyst is the most active among Cu-containing zeolites [1]. Much work of potential relevance to the reaction mechanism has been published [1,3–10]. At the same time, some of these studies have lacks that do not permit to make a final decision on the mechanism.

Witzel et al. reported that H-abstraction from hydrocarbon yielding free radicals is a key step in SCR of NO by propane over transition metal-exchanged ZSM-5 [11]. Among possible transformations of alkyl radicals described in [12], the reaction of propyl radicals with NO (or NO<sub>2</sub>) yielding nitroso- or nitroalkanes should be noted [13]. Several authors have reported those molecules to be the intermediates of the reaction scheme [14–16]. Sachtler proposed a reaction mechanism for NO<sub>x</sub> reduction with propane over Cu-ZSM-5 in the presence of O<sub>2</sub> in which 2-nitrosopropane was the key intermediate [9]. So, there is a set of experimental data suggesting that Cu centers are required to activate hydrocarbon, while metal sites are not directly involved in the interaction of alkyl radicals with NO and following transformations of nitrosopropane because those steps were detected in the absence of Cu over Na-ZSM-5 zeolite [16]. However, in this case the reaction rate was lower than over Cu-ZSM-5, indicating that Cu centers were beneficial for the transformation of intermediates converted into N<sub>2</sub>. In these papers the identification of observed complexes was carried out, but there is no information on their surface coverage. To prove the participation of the surface species in the rate-determining stage, it is necessary to de-

termine kinetic parameters of the adspecies reactions and find a correlation between the dynamics of the surface coverage with surface complexes and steady-state activities of this reaction.

To investigate the nature and kinetics of the surface adspecies transformation, it seems appropriate to use temperature-programmed desorption (TPD). This method does not directly identify the adspecies but the data on the surface coverage can be obtained. The formation of various adspecies formed on the surface of Cu-ZSM-5 with NO and products of its conversion was shown in [17,18] with TPD. We also observed [19] several types of NO and propane adspecies during the reaction over Cu-ZSM-5 catalyst. It was established that the concentration of N-containing species depends on the concentration of reagents and reaction temperature.

A low-exchanged catalyst was used in the present study to simplify the analysis of interconnection of the adspecies coverage with the reaction kinetics because both direct decomposition of NO and SCR of NO with propane occur over excessively exchanged zeolites simultaneously. Meanwhile, there is no NO decomposition over low-exchanged Cu-ZSM-5 zeolite [1] which is the case here. In addition, the NO TPD profiles appear to be simpler, so the peaks could be ascribed more reliably to the decomposition of surface complexes.

In the present study, TPD has been used to further explore the dynamics of the surface processes during the selective reduction of NO with propane over Cu-ZSM-5 catalyst. We tried to detect surface intermediates formed at adsorption and interaction of the reagents over Cu-ZSM-5 and estimate their amount and stoichiometry. Next, the reactivity of absorbed nitrogen- and carbon-containing compounds to O<sub>2</sub> and propane was studied to clarify the active intermediates on the surface. To characterize the specificity of

\* To whom correspondence should be addressed.

the interaction of various adspecies formed in the catalytic reaction, co-adsorption of components has been carried out.

## 2. Experimental

### 2.1. The catalyst preparation

Cu-ZSM-5 ( $\text{Si}/\text{Al} = 19.5$ ) was prepared by traditional ion exchange at  $20^\circ\text{C}$ . A 0.07 M water solution of copper amino complex was added dropwise to a H-ZSM-5 slurry at pH of about 7. The slurry was stirred for 24 h before being vacuum filtered. The product was washed with deionized water. The sample obtained was air dried at  $110^\circ\text{C}$  overnight and then calcined at  $500^\circ\text{C}$  under atmosphere for 4 h. According to the chemical analysis data, the copper content was 1.2 wt% Cu, i.e., exchange level was 56%. BET surface area was  $412\text{ m}^2\text{ g}^{-1}$ . Prior to adsorption/desorption experiments the catalyst was treated in a flow of oxygen for 1 h, followed by a helium one for 1 h at  $500^\circ\text{C}$  repeatedly (about 10 cycles). The catalyst with the particle size of 0.25–0.50 mm was used.

### 2.2. Experimental technique

Prior to the adsorption experiment the sample was pretreated to remove water and adsorbed components from the surface. Two types of sample pretreatment were used: (1) treatment in He flow at  $500^\circ\text{C}$  for 1 h followed by cooling in He to the adsorption temperature, and (2) treatment in oxygen at  $500^\circ\text{C}$  for 1 h followed by cooling in the atmosphere of  $\text{O}_2$ , and then the sample was purged with He flow at the adsorption temperature for 5 min to remove oxygen from the gas phase. The samples are termed as “reduced sample” and “oxidized sample”, respectively. After the pretreatment, the sample was exposed to the flow of appropriate adsorption mixtures, which were prepared with helium dilution of clear gases. After the adsorption equilibrium was reached (usually 20–25 min), the sample was purged with He flow to remove compounds physically adsorbed on the surface. Finally, the programmed heating from the adsorption temperature to  $500^\circ\text{C}$  with the heating rate of  $10^\circ\text{C}/\text{min}$  was started. Some experiments were carried out with the heating rate of 5, 20 or  $25^\circ\text{C}/\text{min}$ . The TPD profiles were recorded in He flow ( $30\text{ cm}^3/\text{min}$ ). All TPD spectra were obtained after the samples pretreatment in He unless otherwise stated.

The TPD profiles of NO and  $\text{NO}_2$  were recorded on an NO– $\text{NO}_2$  gas analyzer Radas-1 (Hartmann & Braun). The accuracy of the NO and  $\text{NO}_2$  measurements is equal to 1 and 4%, respectively. The TPD profiles of  $\text{O}_2$ ,  $\text{N}_2$ ,  $\text{N}_2\text{O}$  and  $\text{NO}_2$  were recorded on three thermoconductivity detectors (TCD) connected consecutively, between which two traps were located to remove components selectively. The first trap was maintained at  $-35 \pm 5^\circ\text{C}$  to remove  $\text{NO}_2$ . The second one was maintained at  $-196^\circ\text{C}$  to remove NO and  $\text{N}_2\text{O}$ . Thus, a full TPD profile was recorded on the

first TCD, the profile without  $\text{NO}_2$  on the second one and TPD of nitrogen and oxygen on the third one. To obtain the individual profiles of  $\text{N}_2$  and  $\text{O}_2$ , periodic tests on those components were carried out followed by the analysis on a Tsvet-500 gas chromatograph with the sampling loop located after the TCD block. The profiles of individual products were obtained by the following processing of the full profile. TPD of  $\text{NO}_2$  was obtained by subtraction of the signal of the second TCD from the signal of the first one. The profile of  $\text{N}_2\text{O}$  was obtained by subtraction of the sums of the third TCD and NO gas-analyzer signals from the signal of the second TCD. All TCD were previously calibrated on  $\text{N}_2$ ,  $\text{O}_2$ ,  $\text{N}_2\text{O}$  by the absolute calibration method, the pathway taken by the gases during the calibration being the same as in the TPD experiments. After the first trap,  $\text{NO}_2$  concentration was beyond detection but 96.5% of  $\text{N}_2\text{O}$  and NO, and more than 99.9% of  $\text{N}_2$  and  $\text{O}_2$  remained in the flow. After the second trap, the concentration of NO and  $\text{N}_2\text{O}$  was beyond detection, however, more than 99.9% of  $\text{N}_2$  and  $\text{O}_2$  remained in the flow. The calibration on NO and  $\text{NO}_2$  was carried out by comparison of the data of TCD and gas analyzer Radas-1. TPD of carbon-containing products were registered with a flame-ionization detector (FID). To analyze propane oxidation products ( $\text{CO}$ ,  $\text{CO}_2$ ), a converter located before FID was used. The converter is a reactor with Ni–Cr reduction catalyst maintained at  $400^\circ\text{C}$  reducing these products to methane in hydrogen flow ( $20\text{ cm}^3/\text{min}$ ). The FID calibration on  $\text{CO}$ ,  $\text{CO}_2$  and  $\text{C}_3\text{H}_8$  was also carried out by the absolute calibration method. To clear He and  $\text{O}_2$  from water vapor, a trap with molecular sieves and a trap filled by stainless steel wire were used, respectively. Both traps were maintained at  $-196^\circ\text{C}$ .

The amount of desorbed gas was calculated from the integral area of the corresponding TPD spectrum. The parameters of individual peaks in TPD profiles such as desorption order, desorption activation energy and pre-exponential factor were calculated by fitting of a simulated curve, which is a superposition of individual peaks, to the experimental one. The peaks were simulated by the Runge–Kutta integration of a system of differential equations describing the desorption and change of the concentration of desorbed products in the gas phase. The desorption activation energy was previously estimated from the equation for the thermodesorption peak maximum [20] assuming a desorption order. Such method for the estimation of the peak parameters is more reliable since the account is made on a large file of experimental data.

## 3. Results and discussion

### 3.1. Co-adsorption of $\text{C}_3\text{H}_8 + \text{NO} + \text{O}_2$

We reported previously [21] on some peaks of the NO desorption in TPD just after SCR of NO with propane in the presence of  $\text{O}_2$ . The TPD profiles after the co-adsorption of NO,  $\text{C}_3\text{H}_8$  and  $\text{O}_2$  on reduced catalyst at  $50^\circ\text{C}$  are similar

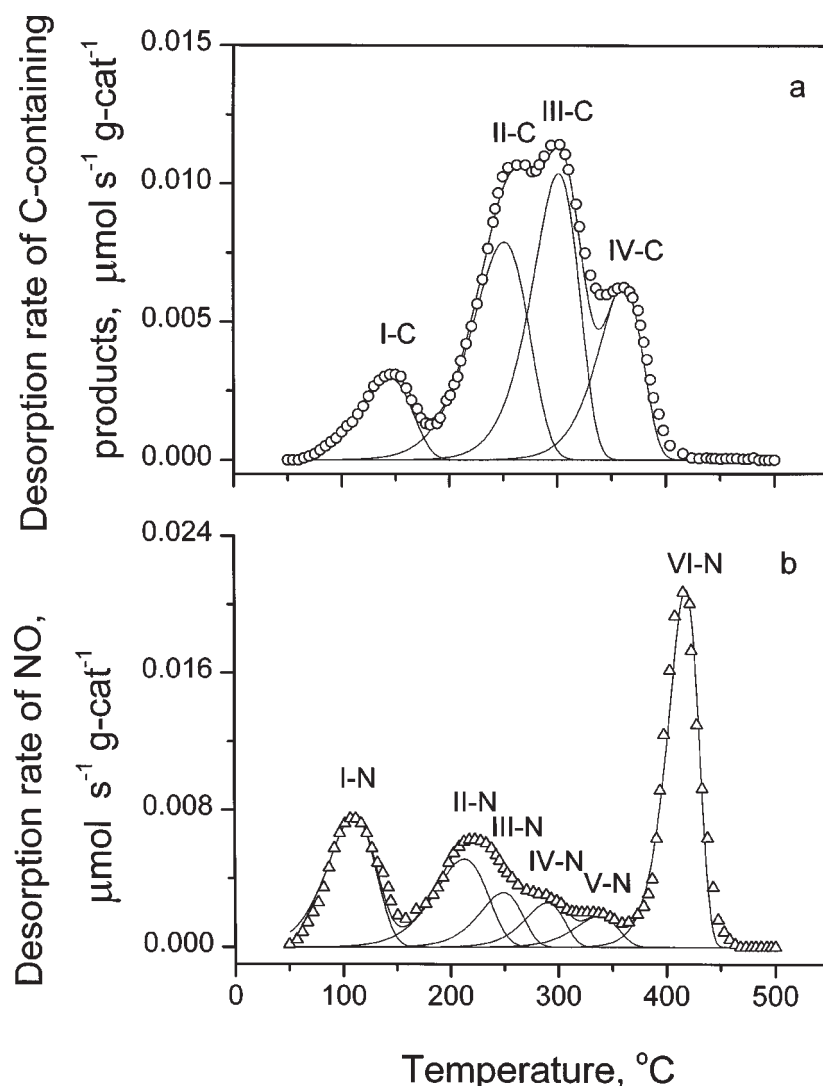


Figure 1. TPD profiles of  $\text{C}_3\text{H}_8$  (a) and  $\text{NO}$  (b) from reduced Cu-ZSM-5 after co-adsorption of  $\text{NO}$  (400 ppm), propane (2000 ppm) and  $\text{O}_2$  (2.2 vol%) at  $50^\circ\text{C}$ . The experimental profiles are plotted as follows: (○) TPD of  $\text{C}_3\text{H}_8$ ; (△) TPD of  $\text{NO}$ . The simulated TPD profiles of individual peaks and sums of them are plotted with solid lines. Heating rate:  $10^\circ\text{C}/\text{min}$ .

to those just after the reaction. Based on the similar character of the desorption spectra obtained at the adsorption of reagents at  $50^\circ\text{C}$  as well as just after the reaction, one may conclude that some adspecies formed after the adsorption are also present on the surface under reaction conditions. There are four desorption peaks of carbon-containing compounds: I-C is propane (peak at about  $145^\circ\text{C}$ ), II-C, III-C, IV-C (peaks at about  $250$ ,  $300$  and  $360^\circ\text{C}$ ) are products of its oxidation:  $\text{CO}$  and  $\text{CO}_2$  (figure 1(a)). The TPD profile of  $\text{NO}$  consists of two desorption peaks at  $110$  and  $415^\circ\text{C}$  with unresolved peaks in between (figure 1(b)). Three shoulders in the TPD profile of  $\text{NO}$  in the range of  $150$ – $350^\circ\text{C}$  are observed. Therefore, the experimental data in this range could be fitted with at least three desorption peaks. However, in this case the fitting curve did not coincide with the experimental data, therefore, four peaks were simulated to obtain a good agreement with the TPD profile. So, six individual peaks at about  $110$ ,  $215$ ,  $250$ ,  $290$ ,  $340$  and  $415^\circ\text{C}$  were detected (peaks from I-N to VI-N in figure 1(b)).

$\text{NO}$  desorption at  $110^\circ\text{C}$  was ascribed to the decomposition of nitrosyls over Cu-ZSM-5 [22,23]. The desorption of  $\text{NO}$  at about  $415^\circ\text{C}$  corresponds to the decomposition of nitrite–nitrate adspecies [22,24]. As the propane concentration increases, the amount of nitrite–nitrate decreases (figure 2(a)). It was ascribed to the formation of N–carbon-containing intermediates [12,13]. Similar data were presented in [25], where decrease in the  $\text{NO}$  amount desorbed from nitrite–nitrate adspecies on Cu-MFI zeolite after addition of propane was reported. In contrast, the amount of nitrite–nitrate adspecies (figure 2(b)) increased after addition of oxygen as well as with the decrease of the adsorption temperature (figure 2(c)). The latter is in accordance with the temperature dependence of  $\text{NO}$  to  $\text{NO}_2$  oxidation reaction rate [26].

The nature of the  $\text{NO}$  peaks from II-N to V-N as well as  $\text{CO}_2$  peaks from II-C to IV-C was not so clear. In order to determine the effect of  $\text{NO}$  on propane adsorption,  $\text{NO}$  was removed from the adsorption mixture.

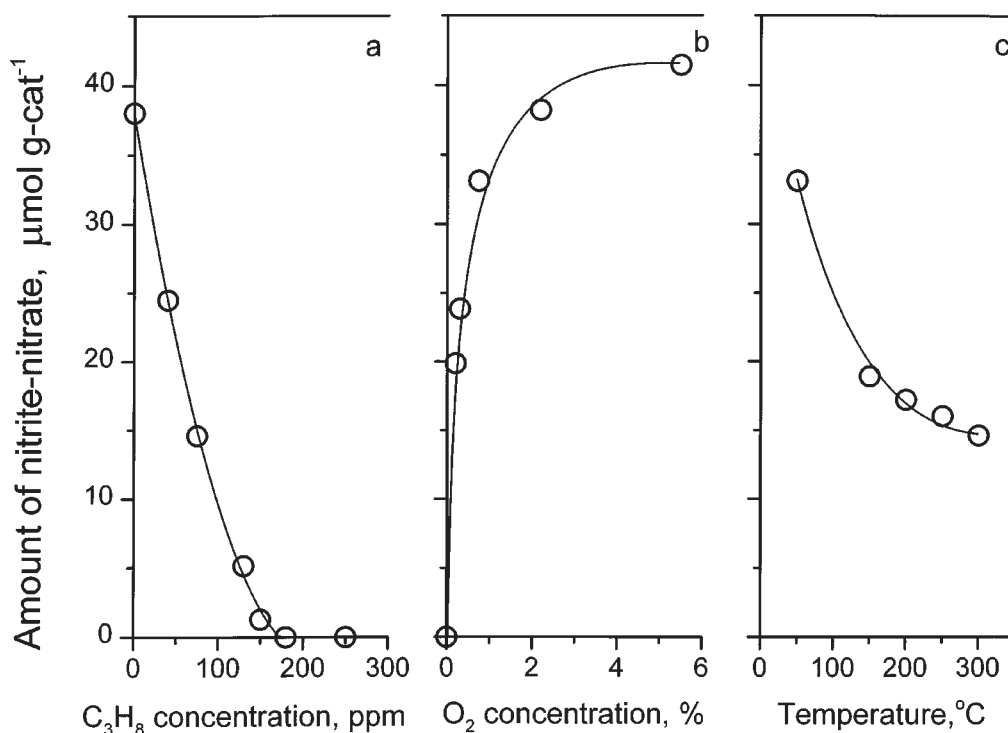


Figure 2. The amount of NO desorbed over reduced Cu-ZSM-5 from nitrite–nitrate adspecies as a function of: (a) C<sub>3</sub>H<sub>8</sub> concentration at 300 °C and 2.2 vol% of O<sub>2</sub>; (b) O<sub>2</sub> concentration at 300 °C, there was no propane added; (c) adsorption temperature at 75 ppm of C<sub>3</sub>H<sub>8</sub>, and 2.2 vol% of O<sub>2</sub>. Concentration of NO was 150 ppm in all experiments.

### 3.2. Co-adsorption of C<sub>3</sub>H<sub>8</sub> + O<sub>2</sub> and adsorption of C<sub>3</sub>H<sub>8</sub>

The TPD profile of C<sub>3</sub>H<sub>8</sub> from reduced Cu-ZSM-5 after co-adsorption of C<sub>3</sub>H<sub>8</sub> and O<sub>2</sub> consists of three individual peaks only; there was no peak II-C at about 250 °C (figure 3(a)). Note that the ratio between the square of peak III-C and peak IV-C is in a direct proportion to the O<sub>2</sub>/C<sub>3</sub>H<sub>8</sub> ratio. The formation of two desorption peaks of the oxygenated products (peaks III-C and IV-C) can be explained by different structure of the adspecies formed. Note, two types of carbon-containing adspecies were observed after adsorption of ethene on Cu-MFI zeolite. One of them is active in the reaction with NO and another is not, but oxygen is effective to increase the amount of the first one [27].

Next, to evaluate the effect of O<sub>2</sub> on the propane adsorption, oxygen was also removed from the adsorption mixture. The TPD profile of C<sub>3</sub>H<sub>8</sub> after adsorption of C<sub>3</sub>H<sub>8</sub> only (figure 3(b)) is similar to that after co-adsorption of C<sub>3</sub>H<sub>8</sub> and O<sub>2</sub>. However, the amount of propane desorbed from peak I-C increased while that of the oxygenated products decreased, as shown in table 1.

We studied [28] the adsorption of propane over H-ZSM-5 zeolite at 50 °C. In this case, a single peak of C<sub>3</sub>H<sub>8</sub> was present in the TPD profile at about 140 °C, while desorption of oxygenated carbon-containing products was not observed. The amount of propane desorbed from H-ZSM-5 was 10.0  $\mu\text{mol g-cat}^{-1}$ , which is comparable with that of the catalyst. This means that the propane adsorption occurs most likely on the zeolite rather than on Cu sites. The high-

temperature shift of the propane desorption peak appears to be due to changes in the structure of propane adsorption centers when Cu is not present in the zeolite.

So, TPD results on Cu-ZSM-5 indicated that the presence of NO in the adsorption mixture was responsible for peak II-C. To evaluate the effect of NO on the adsorption of propane, TPD of both C<sub>3</sub>H<sub>8</sub> and NO after co-adsorption of NO and C<sub>3</sub>H<sub>8</sub> was carried out.

### 3.3. Co-adsorption of C<sub>3</sub>H<sub>8</sub> + NO and adsorption of NO

The TPD profile of propane from reduced Cu-ZSM-5 catalyst after co-adsorption of NO and C<sub>3</sub>H<sub>8</sub> is plotted in figure 4(a). Note that peak II-C as well as peaks I-C, III-C and IV-C are present in the TPD profile of C<sub>3</sub>H<sub>8</sub>. The TPD profile of NO after the co-adsorption of NO and C<sub>3</sub>H<sub>8</sub> consists of three individual peaks only (figure 4(b)). In addition to peaks I-N and VI-N, NO peak III-N at about 250 °C was observed. Note that as the propane concentration increases, the desorption of NO from peak III-N gradually increases while that from nitrite–nitrate decreases. Ultimately, there is no NO desorption from nitrite–nitrate at 2000 ppm of propane. However, the increase in the NO concentration leads either to an increase or a decrease in the amount of this complex depending on NO concentrations (see table 1).

To evaluate the nature of peak III-N, the NO TPD was carried out as a blank experiment. After exposure of the reduced catalyst to NO at 50 °C, two desorption peaks I-N and VI-N at about 100 and 415 °C, respectively, were observed. The profile of NO is similar to that in [24,29]. There was no

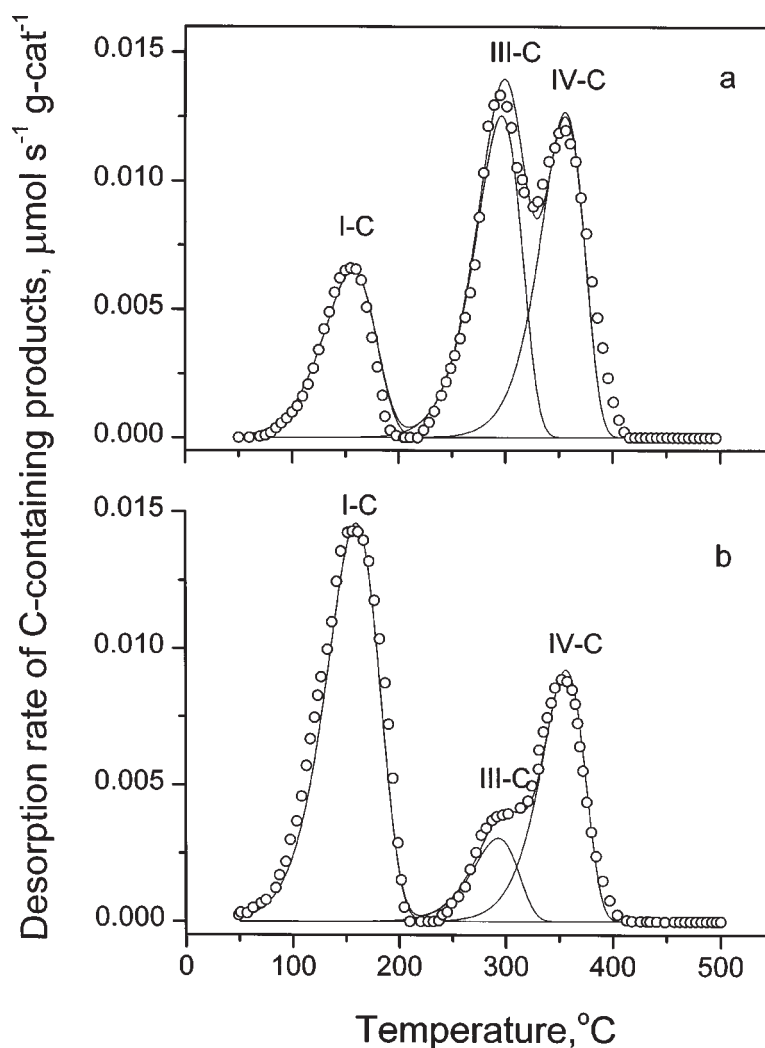


Figure 3. TPD profiles of C<sub>3</sub>H<sub>8</sub> from reduced Cu-ZSM-5: (a) after co-adsorption of C<sub>3</sub>H<sub>8</sub> (110 ppm) and O<sub>2</sub> (2.2 vol%) at 50 °C; (b) after adsorption of C<sub>3</sub>H<sub>8</sub> (110 ppm) at 50 °C. The experimental and simulated TPD profiles are plotted as in figure 1. Heating rate: 10 °C/min.

Table 1  
Product distribution in the TPD experiments over reduced Cu-ZSM-5 catalyst.<sup>a</sup>

Concentrations of gases adsorbed			Heating rate (°C/min)	Amount <sup>b</sup> of gases desorbed in peaks					CO <sub>2</sub> /NO in peak J
NO (ppm)	C <sub>3</sub> H <sub>8</sub> (ppm)	O <sub>2</sub> (vol%)		I-C <sup>c</sup>	II-C (J) <sup>d</sup>	III-C <sup>d</sup>	IV-C <sup>d</sup>	III-N (J) <sup>e</sup>	
400	2000	2.20	10	1.2	3.2	3.5	2.0	1.03	3.1
–	110	2.20	10	2.5	–	4.2	3.8	–	–
–	110	–	10	5.7	–	1.0	2.9	–	–
400	110	–	10	1.4	1.2	1.3	0.7	0.41	2.9
150	2000	–	10	4.2	1.0	2.3	1.2	0.34	2.9
400	2000	–	10	1.9	3.0	3.2	1.9	1.01	3.0
1400	2000	–	10	1.3	1.8	4.0	2.2	0.61	3.0
400	2000	–	5	2.0	3.0	3.3	2.0	0.94	3.2
400	2000	–	20	2.1	2.9	3.1	2.0	0.97	3.0

<sup>a</sup>The data of table 1 were calculated based on separation of the C<sub>3</sub>H<sub>8</sub> TPD profiles on individual desorption peaks with computer of processing of experimental profiles. The activation energies and pre-exponential factors of peaks are summarized in table 2. <sup>b</sup>μmol g-cat<sup>-1</sup>. <sup>c</sup>C<sub>3</sub>H<sub>8</sub>. <sup>d</sup>CO<sub>2</sub>. <sup>e</sup>NO.

desorption of NO<sub>2</sub> as well as in the NO TPD experiments of Iwamoto et al. [30] and Li and Armor [24]. However, in contrast to TPD from over-exchanged Cu-ZSM-5 catalysts, in our case the low-temperature desorption of NO was rather small. Another important feature that should be noted is that unusually large desorption of N<sub>2</sub>O at about 220, 270

and 320 °C was observed for low-exchanged Cu-ZSM-5, which was ascribed to the decomposition of NO adspecies yielding N<sub>2</sub>O as shown in the appendix in detail.

In summary, the absence of peak III-N in the NO TPD profiles suggests that only propane and NO are required to form it while oxygen is not necessary.

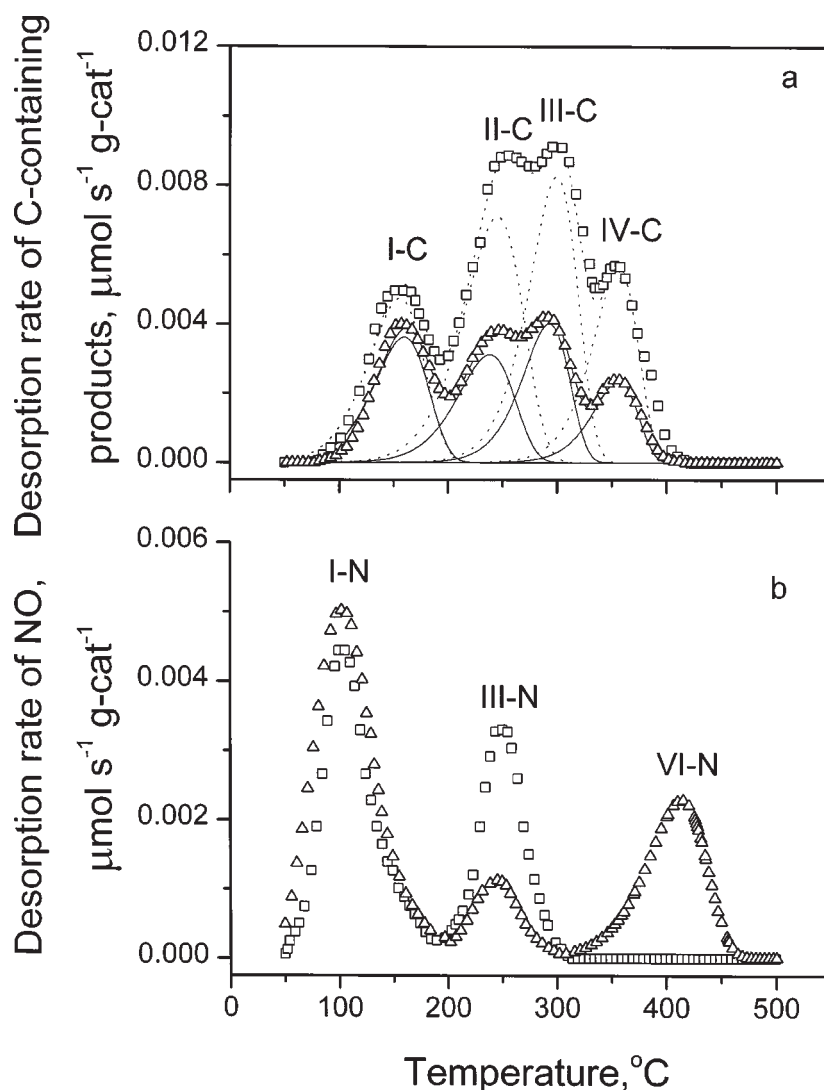


Figure 4. TPD profiles of  $\text{C}_3\text{H}_8$  (a) and  $\text{NO}$  (b) from reduced Cu-ZSM-5 after co-adsorption of  $\text{NO}$  (400 ppm) and  $\text{C}_3\text{H}_8$  (110 or 2000 ppm). The experimental profiles are plotted as follows: ( $\Delta$ ) for 110 ppm of  $\text{C}_3\text{H}_8$ ; ( $\square$ ) for 2000 ppm of  $\text{C}_3\text{H}_8$ . Simulated TPD profiles of individual peaks and sums of them are plotted with solid lines for 110 ppm of  $\text{C}_3\text{H}_8$  and dotted lines for 2000 ppm of  $\text{C}_3\text{H}_8$ . Heating rate:  $10^\circ\text{C}/\text{min}$ .

As shown earlier, the maxima of peaks III-N and II-C are very close to each other (figure 4). This fact can be caused by several factors. First, an interaction of  $\text{NO}$  and  $\text{C}_3\text{H}_8$  may occur on the catalyst surface forming an intermediate which consists of both  $\text{NO}$  and carbon-containing fragments. On the other hand, on addition of propane to the adsorption mixture, the state of  $\text{NO}$  adsorption centers can be also changed and, as a result, it can bring into existence new peaks of the  $\text{NO}$  desorption and only casual concurrence of the maximum of peak III-N with that of peak II-C. In order to investigate the nature of those peaks, both  $\text{NO}$  and  $\text{C}_3\text{H}_8$  TPD experiments were carried out at different heating rates (5, 10,  $20^\circ\text{C}/\text{min}$ ). Some of the TPD profiles are presented in figure 5. The temperature of maxima of peaks II-C, III-C, IV-C as well as that of peak III-N decreases in going from the heating rate of 20 to  $5^\circ\text{C}/\text{min}$ . The resolution improvement of peaks in the TPD profile of propane obtained at  $5^\circ\text{C}/\text{min}$  makes possible a more reliable simulation of peak II-C and the whole profile as well.

As demonstrated in figure 5, a good fit of simulated curves to the experimental data is observed for all heating rates. The fitting parameters employed are presented in table 2. Note that the parameters of peaks II-C, III-C and IV-C were the same except for the heating rate.

The maximum of peak III-N coincides with that of peak II-C for all heating rates. This uniquely testifies that a surface complex containing both  $\text{NO}$  and carbon-containing fragments decomposed at this interval of temperatures. Peaks III-N and II-C in both TPD of  $\text{NO}$  and propane relating to the decomposition of this intermediate will be denoted as peak J (joint) hereafter.

The surface coverage with various adspecies is presented in table 1. The  $\text{CO}_2/\text{NO}$  ratio in peak J is close to 3. This ratio was accurate to within 7% because the accuracy of the amount of  $\text{NO}$  desorption calculated from the TPD data was 2% according to the  $\text{NO}$  detection validity, and that of the amount of  $\text{CO}_2$  desorbed was 5% according to the accuracy of the separation of the TPD profile on

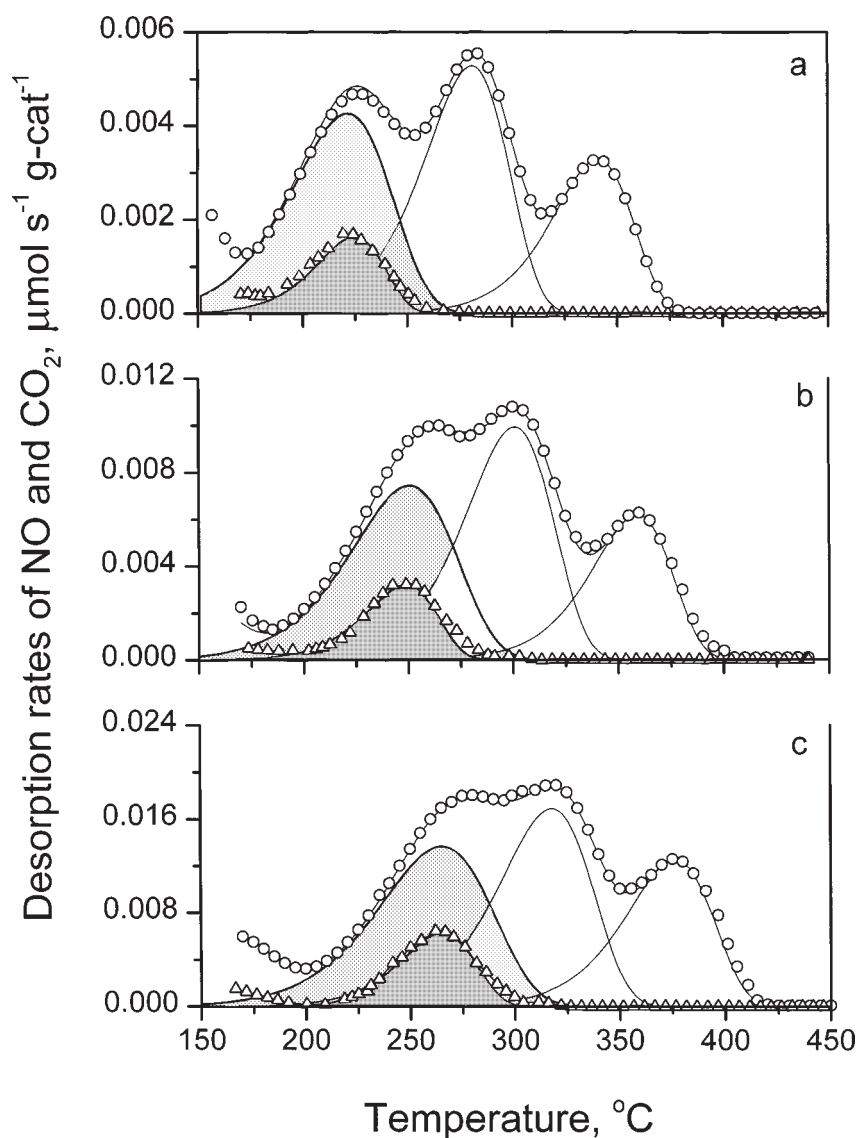


Figure 5. Some of the TPD profiles of NO and CO<sub>2</sub> from reduced Cu-ZSM-5 between 150 and 450 °C after co-adsorption of NO (400 ppm) and C<sub>3</sub>H<sub>8</sub> (2000 ppm) at 50 °C at different heating rates: (a) 5 °C/min; (b) 10 °C/min; (c) 20 °C/min. The experimental and simulated TPD profiles are plotted as in figure 1. The joint peak J is filled with gray color.

Table 2  
Parameters<sup>a</sup> employed for the simulation of individual desorption peaks.

Concentrations of gases adsorbed			Heating rate (°C/min)	Activation energy employed for the simulation of peaks (kcal/mol)									
NO (ppm)	C <sub>3</sub> H <sub>8</sub> (ppm)	O <sub>2</sub> (vol%)		I-C <sup>b</sup>	II-C <sup>c</sup>	III-C <sup>c</sup>	IV-C <sup>c</sup>	I-N <sup>d</sup>	II-N <sup>c</sup>	III-N <sup>c</sup>	IV-N <sup>c</sup>	V-N <sup>c</sup>	VI-N <sup>e</sup>
400	2000	2.20	10	12.8	25.8	28.6	31.9	15.0	23.9	25.9	28.3	30.8	41.2
–	110	2.20	10	13.4	–	28.5	32.0	–	–	–	–	–	–
–	110	–	10	13.4	–	28.5	32.0	–	–	–	–	–	–
400	110	–	10	13.4	26.0	28.5	32.0	14.8	–	26.0	–	–	–
400	2000	–	5	13.4	26.0	28.5	32.0	15.0	–	26.0	–	–	–
400	2000	–	10	13.4	26.0	28.5	32.0	15.0	–	26.0	–	–	–
400	2000	–	20	13.4	26.0	28.5	32.0	15.0	–	26.0	–	–	–
400	–	–	20	–	–	–	–	14.8	–	–	–	–	41.3
400	–	2.20	20	–	–	–	–	14.2	–	–	–	–	41.3

<sup>a</sup>Parameters of peaks were calculated based on the first order of desorption. The first order was chosen, since the maxima peaks were not changed at various surface coverage with carbon-containing adspecies. <sup>b</sup>Pre-exponential factor equals  $1.0 \times 10^5 \text{ s}^{-1}$ . <sup>c</sup>Pre-exponential factor equals  $1.0 \times 10^{11} \text{ s}^{-1}$ .

<sup>d</sup>Pre-exponential factor equals  $1.0 \times 10^9 \text{ s}^{-1}$ . <sup>e</sup>Pre-exponential factor equals  $1.0 \times 10^{13} \text{ s}^{-1}$ .

individual peaks because the difference in the  $\text{CO}_2$  amount obtained at different heating rates did not exceed 5%. So, the  $\text{CO}_2/\text{NO}$  ratio equals  $3.0 \pm 0.2$  at various compositions of the adsorption mixture and various heating rates of the catalyst. According to this fact, one may assume that peak J corresponds to the decomposition of a surface intermediate which consists of NO and three carbon atoms. Among N-carbon-containing compounds described in the literature [13,31–33], only nitrosopropane has the ratio of  $\text{C}/\text{N} = 3$  and can decompose yielding NO rather than  $\text{N}_2\text{O}$  or  $\text{N}_2$ . The fact that the increase in the NO concentration results, first, in the increase in the square of peak J, and then, in its decrease, suggests that the surface complex can react with NO yielding other intermediates which are not observed in TPD.

From the above experiments, it can be concluded that peak J can be assigned to the decomposition of a surface

complex like nitrosopropane. At the same time the absence of peaks II-N, IV-N, V-N at the co-adsorption of NO and  $\text{C}_3\text{H}_8$  means that oxygen is required to form them. To support our conclusion, the co-adsorption of NO and  $\text{C}_3\text{H}_8$  was carried out on the oxidized sample followed by the TPD of NO. In this case, the TPD profile consisted of six NO peaks; their positions were the same as those after co-adsorption of  $\text{NO} + \text{C}_3\text{H}_8 + \text{O}_2$ . However, the amount of nitrite–nitrate was lower than after the co-adsorption of three components. This result may suggest that some oxidation of the catalyst is required to form surface species indicated by the appearance of three TPD peaks in the range from 150 to  $400^\circ\text{C}$ . To investigate further the nature of the formation of the above mentioned NO peaks and evaluate the effect of oxygen on their formation,  $\text{O}_2$  TPD experiments were performed after the  $\text{O}_2$  adsorption and co-adsorption of NO and  $\text{O}_2$ .

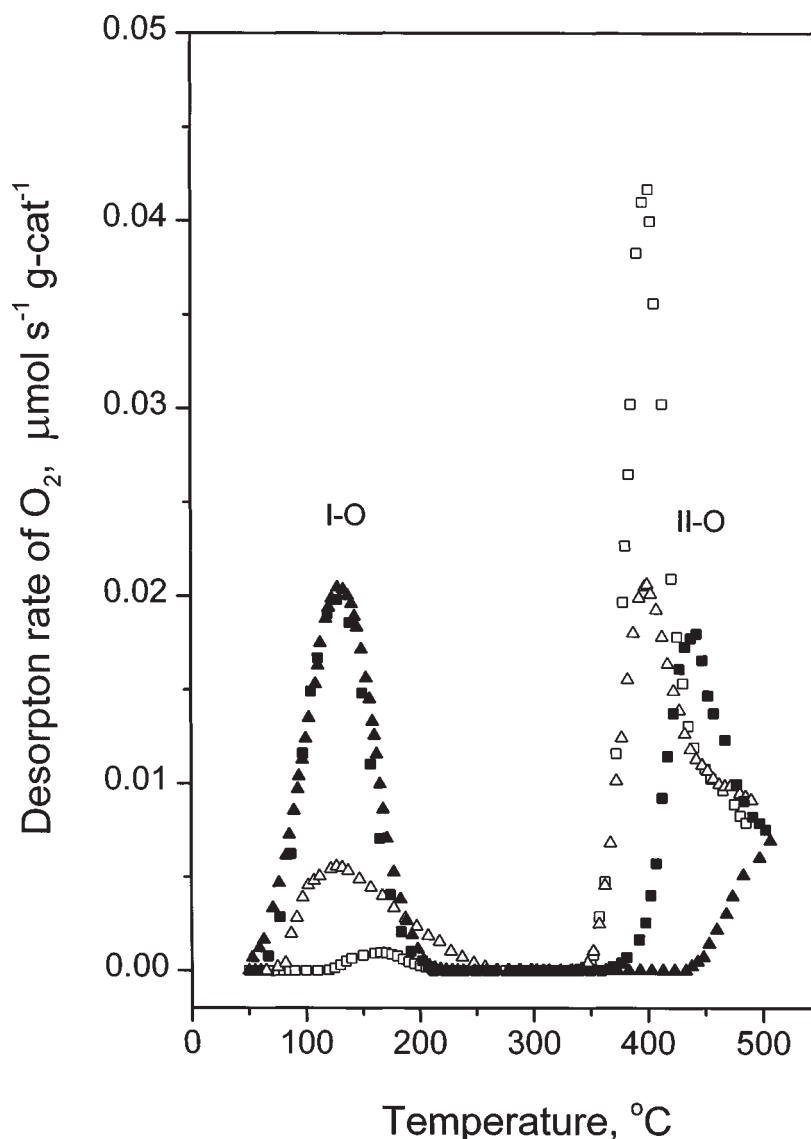


Figure 6. TPD profiles of  $\text{O}_2$  from reduced Cu-ZSM-5 after: (▲)  $\text{O}_2$  adsorption at  $50^\circ\text{C}$ ; (■)  $\text{O}_2$  adsorption at  $500^\circ\text{C}$ .  $\text{O}_2$  concentration for adsorption was 2.2 vol%. TPD profiles of  $\text{O}_2$  from Cu-ZSM-5 after adsorption of  $\text{O}_2$  (2.2 vol%) and NO (400 ppm): (Δ) the reduced sample was saturated with oxygen at  $50^\circ\text{C}$  followed by the NO adsorption at  $50^\circ\text{C}$ ; (□) NO was adsorbed at  $50^\circ\text{C}$  on the oxidized sample. Heating rate:  $10^\circ\text{C}/\text{min}$ .

### 3.4. Adsorption of $\text{O}_2$ and co-adsorption of $\text{NO} + \text{O}_2$

As the initial H-ZSM-5 does not show any oxygen desorption peaks, the adsorption of oxygen on Cu-ZSM-5 was ascribed to the presence of copper ions. The TPD profile of  $\text{O}_2$  depends on the adsorption temperature, as shown in figure 6. When oxygen was adsorbed at  $50^\circ\text{C}$ , at least two different states of oxygen on the surface were present, indicated by two TPD peaks at about  $130^\circ\text{C}$  (peak I-O) and above  $450^\circ\text{C}$  (peak II-O). In the TPD of  $\text{O}_2$  after adsorption at  $500^\circ\text{C}$ , the desorption peak I-O was also observed at the same position but the maximum of peak II-O was at about  $440^\circ\text{C}$ .

The first peak was assigned to the associative oxygen adsorption [37]. The amount of oxygen desorbed from peak I-O is  $0.045 \text{ O}_2/\text{Cu}$ . It is interesting to note that as the exchange level increases, the amount of copper centers available for associative oxygen adsorption also increases: 20% of Cu for the exchange level of 114%,  $\text{Si}/\text{Al} = 14$  [38], 17% of Cu for the exchange level of 103%,  $\text{Si}/\text{Al} = 17$  [37] and 4.5% of Cu for the exchange level of 56%,  $\text{Si}/\text{Al} = 19.5$ . One can see from figure 7 that the surface coverage with molecularly adsorbed oxygen at  $50^\circ\text{C}$  was practically complete at about 0.2 vol% of  $\text{O}_2$ . The constant of oxygen adsorption equilibrium is  $4.0 \times 10^4 \text{ atm}^{-1}$ . So, the desorption activation energy and pre-exponential factor ( $k$ ) are equal to  $11.4 \text{ kcal/mol}$  and to  $1.0 \times 10^6 \text{ s}^{-1}$ , respectively.

Peak II-O was assigned to the dissociative oxygen adsorption [37]. Indeed, its maximum shifted in the lower temperature region after adsorption at  $500^\circ\text{C}$  when the

surface coverage with atomic oxygen was expected to be higher than that at  $50^\circ\text{C}$ . The difference of the low-exchanged catalyst from over-exchanged ones is in the fact that oxygen is adsorbed in the molecular form even at  $500^\circ\text{C}$  while on over-exchanged zeolites the adsorption occurs mainly in the atomic form [37]. It is known that the oxygen adsorption on over-exchanged Cu-ZSM-5 occurs, either in the molecular form or in the atomic one, on the same type of copper centers, depending on the adsorption temperature. However, in our case the adsorption in the molecular form occurs on the surface centers of another type different from those on which the adsorption of the atomic form takes place. This conclusion follows from the fact that the amount of the molecular form of oxygen does not depend on the adsorption temperature while that of the atomic form changes significantly.

Thus, the amount of atomic oxygen, which can be responsible for the formation of N-containing surface compounds indicated by the appearance of three peaks II-N, IV-N and V-N after the pretreatment of the catalyst in oxygen, increased on oxidized catalysts in comparison with the reduced one.

To study the reactivity of oxygen adspecies to NO, the reduced sample was saturated with oxygen at  $50^\circ\text{C}$  followed by the NO adsorption at  $50^\circ\text{C}$ . In this case, the high-temperature  $\text{O}_2$  desorption was changed (figure 6): there was a maximum at about  $400^\circ\text{C}$  and a tailing part, which appears to correspond to the evolution of oxygen adsorbed in the atomic form (peak II-O). The square of peak I-O decreased. This is caused by the fact that the NO adsorption

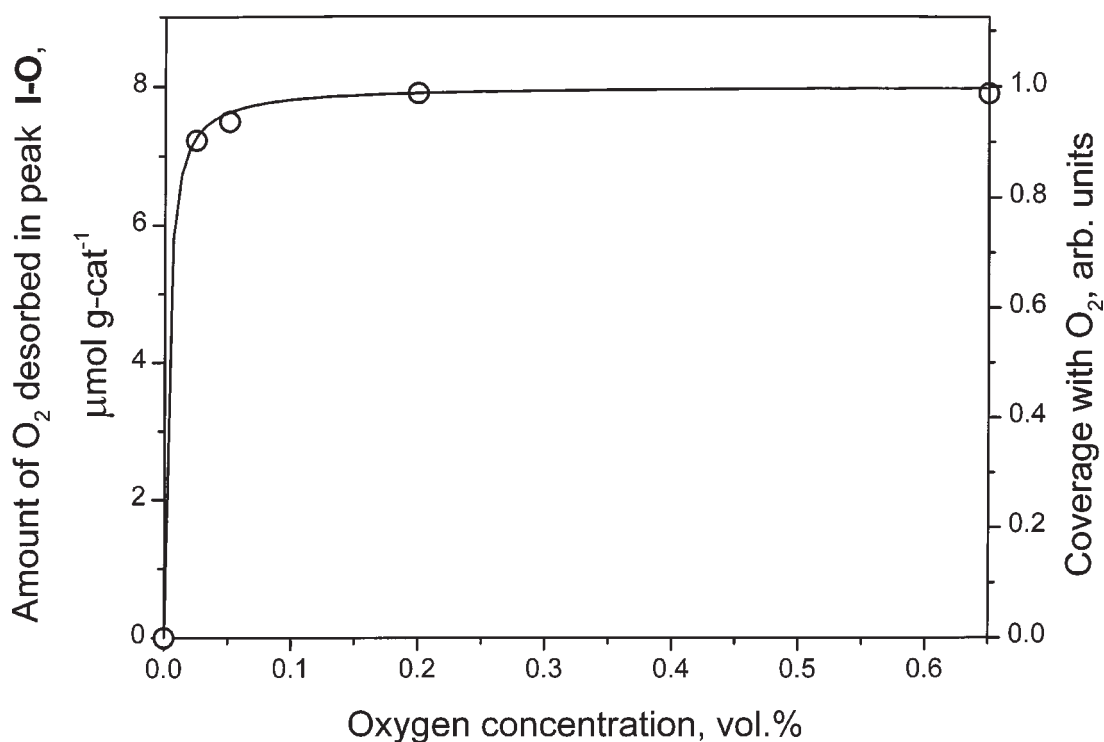


Figure 7. The isotherm of the oxygen adsorption in the molecular form at  $50^\circ\text{C}$ . Experimental data are plotted with circles; data calculated by the Langmuir equation are plotted with a solid line.

Table 3  
The distribution of NO desorbed from nitrosyl and nitrite–nitrate species in the TPD experiments over reduced Cu-ZSM-5 catalyst.

Content in the feed gas during adsorption		Adsorption temperature (°C)	Amount <sup>a</sup> of NO desorbed from		
NO (ppm)	O <sub>2</sub> (vol%)		nitrosyl	nitrite–nitrate	total
190	2.5	50	7.7	30.4	38.1
190	5.9	50	3.6	36.8	40.4
190	11.0	50	0.2	43.4	43.6
470	11.0	50	0.0	49.2	49.2
870	11.0	50	0.0	49.3	49.3
150	–	50	0.7	1.8	2.5
480	–	50	2.1	4.8	6.9
480	–	29	1.4	12.1	13.5
480	–	0	0.9	30.0	30.9
1400	–	50	8.7	12.9	21.6
3400	–	50	16.0	21.0	37.0

<sup>a</sup> μmol g-cat<sup>−1</sup>.

occurs on the same surface centers as those on which oxygen adsorption does [37]. The evolution of oxygen with a peak at about 400 °C was ascribed to the NO decomposition [37]. The NO TPD profile after a step-by-step adsorption of O<sub>2</sub> and NO consists of two peaks I-N and VI-N at about 80 and 415 °C, respectively. The desorption of NO from nitrosyls is shifted to lower temperature in comparison with that without oxygen because some oxidation of Cu<sup>+</sup> to Cu<sup>2+</sup> occurs with oxygen [34] while Cu<sup>+</sup> ions adsorb NO much more strongly [35]. The ratio between peaks I-N and VI-N depends on the oxygen concentration during the adsorption, as shown in table 3.

As the oxygen concentration increases, the amount of NO desorbed from nitrite–nitrate also increases but that desorbed from nitrosyl decreases in the same manner as in [36]. Based on the data of table 3, one can see that the total amount of N-containing adspecies remains approximately the same in going from 2.5 to 11.0 vol% of O<sub>2</sub> and constant NO concentration. This data suggests that the adsorption of nitrosyl and nitrite–nitrate occurs on the same surface center just as it does on over-exchanged Cu-ZSM-5 [37]. Note that when NO was present in the adsorption mixture only, an increase of the NO concentration leads to an increase of the amount of NO desorbed from nitrite–nitrate (see table 3) due to the oxidation of the surface during the decomposition of di-nitrosyls formed at higher NO concentrations [39,40].

From table 3 one can see that the total coverage with nitrite–nitrate is close to 49.3 μmol g-cat<sup>−1</sup>. Thus, the amount of NO desorbed from them is 0.27 NO/Cu. This result indicates that only 27% of the copper centers are active in the NO adsorption at 50 °C, whereas only 5% of them are active in the associative oxygen adsorption. The relatively small amount of oxygen desorbed at 400 °C in comparison to that of adsorbed NO indicates that there is little NO decomposition proceeding on the low-exchanged sample, and as a result, the catalyst was in a reduced state even being exposed to the mixture having the NO concentration as low as 400 ppm. Another conclusion may also be reached that peaks II-N, IV-N and V-N are only formed

when both NO and C<sub>3</sub>H<sub>8</sub> are absorbed on the “oxidized” catalyst. To maintain the catalyst in the oxidized state, oxygen in the gas phase or an oxygen pretreatment is required.

#### 4. Conclusions

Our study revealed that the peculiarities of the interaction of propane, oxygen and NO over low-exchanged Cu-ZSM-5 are in many respects similar to those observed over excessively exchanged ones. However, the low-exchanged Cu-ZSM-5 catalyst has some characteristic features. Among them, a substantial amount of propane adsorbed in the molecular form, which is held on Cu-ZSM-5 as well as on the initial H-ZSM-5 up to 150 °C. The amount of oxygen in the molecular form depends on the exchange level but not on the adsorption temperature. The total coverage with the molecularly adsorbed oxygen has been reached at a very low O<sub>2</sub> concentration in the feed. Other feature of the low-exchanged catalyst is the absence of the NO<sub>2</sub> desorption and large desorption of N<sub>2</sub>O after adsorption of NO. The latter is due to some types of adsorbed NO decomposing with the N<sub>2</sub>O formation on Cu<sup>+</sup> cations and mainly on Fe<sup>2+</sup> impurities.

Some adspecies of a complex structure have been observed after propane and oxygen interaction with NO over Cu-ZSM-5. Their amount depends on both the initial condition of the catalyst surface and concentrations of the reagents. The kinetics of the nitrite–nitrate formation and decomposition as a function of propane and oxygen concentrations and temperature has been determined.

It is of prime importance that the stoichiometry of one of the adspecies is close to that of nitrosopropane. It is known that nitrosopropane is not stable, however, the choice of appropriate adsorption conditions made it possible to define the surface coverage of them and to observe products of its decomposition in the TPD profiles of NO and CO<sub>2</sub> over Cu-ZSM-5 catalyst. The amount of this complex was relatively small (about 1.0 μmol g-cat<sup>−1</sup>). As the propane concentration increases the amount of this complex also increases, while the increase in the O<sub>2</sub> concentration results

in the decrease in their amount. However, the increase in the NO concentration lead either to the increase or decrease in the amount of this complex depending on the concentrations of the reagents. This indicates that the surface complex reacting with  $\text{O}_2$  and NO can transform to other surface substances. In order to obtain more reliable evidence of the interaction between N–C adspecies and/or NO other techniques should be applied. This work is now in progress.

## Appendix

Unusually intensive desorption of  $\text{N}_2\text{O}$  at about 220, 270 and 320 °C was observed in TPD profiles of  $\text{N}_2\text{O}$  after the NO adsorption on reduced Cu-ZSM-5 (figure 8(c)). This may be ascribed to some types of absorbed NO yielding

$\text{N}_2\text{O}$  rather than NO at decomposition. To study surface adspecies yielding  $\text{N}_2\text{O}$  as well as  $\text{N}_2$  at decomposition, a set of TPD experiments of both  $\text{N}_2\text{O}$  and  $\text{N}_2$  over Cu-ZSM-5 and H-ZSM-5 was carried out after the NO adsorption and the co-adsorption of NO with propane and/or oxygen. The experimental profiles and simulated ones are presented in figures 8 and 9 for  $\text{N}_2\text{O}$  and  $\text{N}_2$ , respectively. The  $\text{N}_2\text{O}$  TPD profiles were divided into seven individual peaks according to their maxima, the ratio of them depending on the ratio of  $\text{C}_3\text{H}_8/\text{O}_2$  in the adsorption mixture and the catalyst pretreatment as well. The data on the amount of  $\text{N}_2\text{O}$  and  $\text{N}_2$  desorbed from each peak are presented in table 4, and parameters of peaks in table 5 for the zeolite and the catalyst.

A single peak of the  $\text{N}_2\text{O}$  desorption at about 135 or 170 °C was observed after its adsorption on the zeolite or

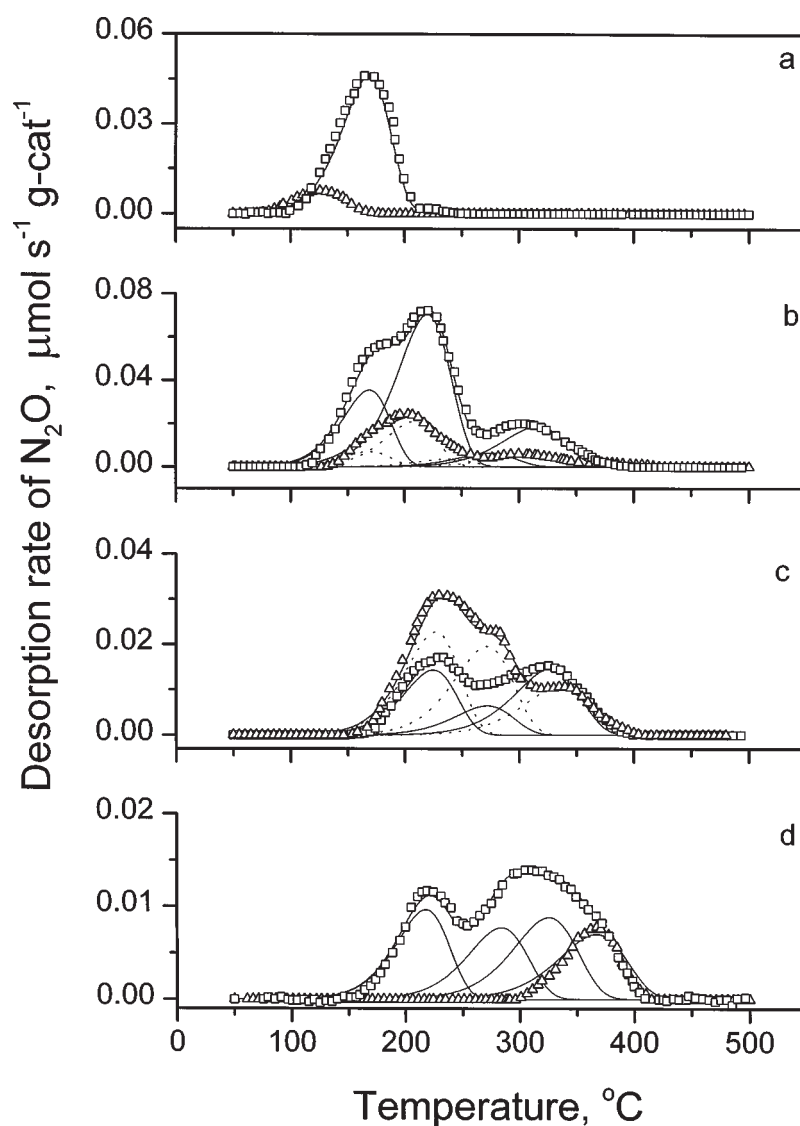


Figure 8. TPD profiles of  $\text{N}_2\text{O}$  from reduced H-ZSM-5 and reduced Cu-ZSM-5 after adsorption of mixtures of components except for case (a) when 5 pulses of 100  $\mu\text{l}$  of pure  $\text{N}_2\text{O}$  were passed through the sample. The mixture composition was as follows: (b) 400 ppm of NO and 2000 ppm of  $\text{C}_3\text{H}_8$ ; (c) 400 ppm of NO; (d) 400 ppm of NO and 2.2 vol% of  $\text{O}_2$ . The experimental profiles are plotted as follows: ( $\Delta$ ) for H-ZSM-5; ( $\square$ ) for Cu-ZSM-5. Simulated TPD profiles of individual peaks and the sums of them are plotted with solid lines for Cu-ZSM-5 and dotted lines for H-ZSM-5. Adsorption temperature: 50 °C. Heating rate: 20 °C/min.

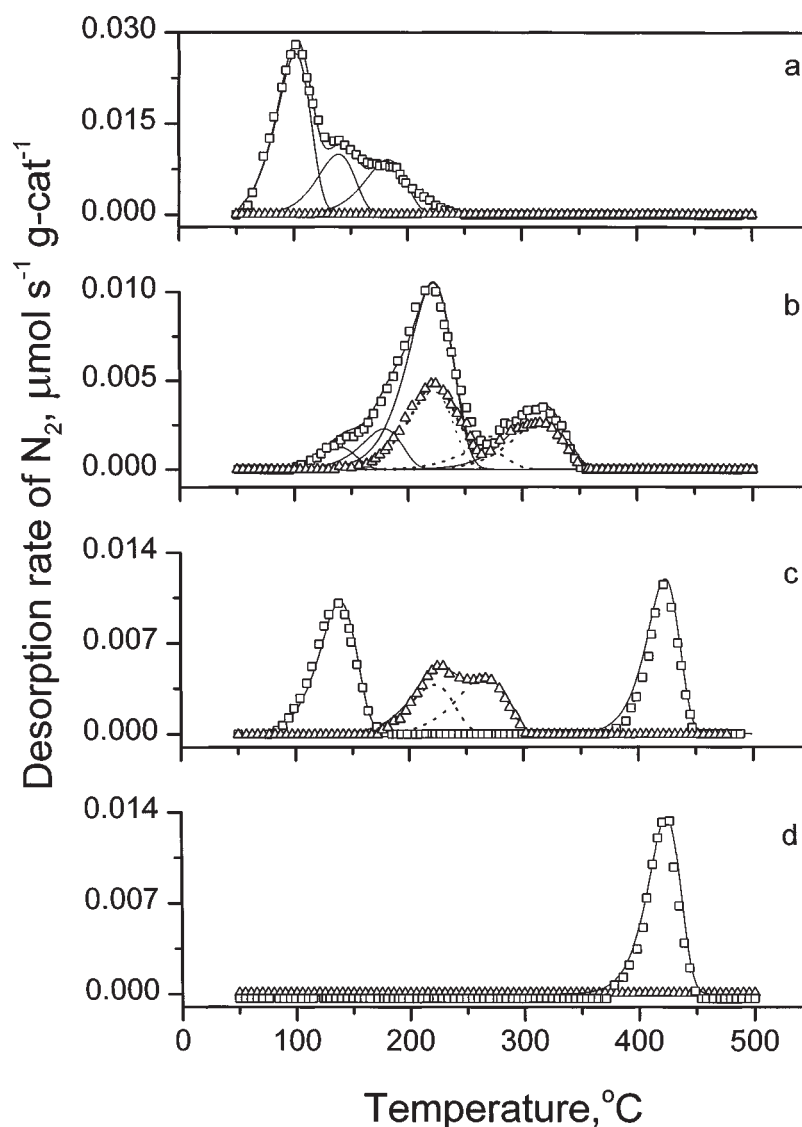


Figure 9. TPD profiles of  $\text{N}_2$  from reduced H-ZSM-5 and reduced Cu-ZSM-5. The adsorption mixtures, adsorption temperature, and heating rate were the same as in figure 8. The experimental profiles are plotted as follows: ( $\Delta$ ) for H-ZSM-5; ( $\square$ ) for Cu-ZSM-5. Simulated TPD profiles of individual peaks and the sums of them are plotted with solid lines for Cu-ZSM-5 and dotted lines for H-ZSM-5.

the catalyst, respectively (figure 8(a)). The total amount of nitrous oxide desorbed from the catalyst surface is  $0.048 \text{ N}_2\text{O}/\text{Cu}$ . The reduction of some copper cations at the co-adsorption of  $\text{C}_3\text{H}_8$  and  $\text{NO}$  appears to be responsible for the readsorption of nitrous oxide indicated by  $\text{N}_2\text{O}$  desorption peak III, similar with that in the  $\text{N}_2\text{O}$  TPD profile after the  $\text{N}_2\text{O}$  adsorption. Peaks IV–VII can be ascribed to several types of centers of the  $\text{NO}$  adsorption on metal cations with a different spatial arrangement [41]. Note that after the  $\text{NO}$  adsorption, the total amount of  $\text{N}_2\text{O}$  desorbed from H-ZSM-5 was nearly 1.5 times higher than that from the catalyst, desorption from the zeolite in peak V being more than five times more intensive than that from the catalyst.

According to the chemical analysis data, H-ZSM-5 zeolite contains about 0.09 wt% Mg, Ca and Fe. The latter is already present in the zeolite as a result of the synthesis in Fe-containing apparatus. Fe actions are known to be active

in the conversion of nitrogen oxides [42]. In our case, the transformation of  $\text{NO}$  also appears to occur on Fe ions because the total amount of  $\text{N}_2\text{O}$  and  $\text{N}_2$  desorbed from the zeolite ( $13.4 \pm 1.0 \text{ } \mu\text{mol g-cat}^{-1}$ ) correlates well with the Fe content ( $16.0 \pm 1.8 \text{ } \mu\text{mol g-cat}^{-1}$ ).

The desorption of  $\text{N}_2\text{O}$  from the catalyst was accompanied by the nitrogen desorption (figure 9(a)), which can be divided into three individual peaks at  $100^\circ\text{C}$  (peak I),  $135^\circ\text{C}$  (peak II) and  $160^\circ\text{C}$  (peak III). It is well known that the  $\text{N}_2$  formation accompanying the reoxidation of reduced surface copper centers occurs as a result of the  $\text{N}_2\text{O}$  adsorption on  $\text{Cu}^+$  ions [43]. The complex  $\text{N}_2$  desorption peak seems to be related to the variety of Cu and Fe centers participating in the  $\text{N}_2\text{O}$  decomposition reaction on the Cu-ZSM-5 catalyst.

The desorption peak of  $\text{N}_2$  at about  $135^\circ\text{C}$  was ascribed to the decomposition of  $\text{N}_2\text{O}$  because it was observed in

Table 4  
N<sub>2</sub>O and N<sub>2</sub> distribution in the TPD experiments over reduced Cu-ZSM-5 and reduced H-ZSM-5.

Gases adsorbed <sup>a</sup>	Product distribution <sup>a</sup>															
	N <sub>2</sub> O (μmol g-cat <sup>-1</sup> )								N <sub>2</sub> (μmol g-cat <sup>-1</sup> )							
	I	II	III	IV	V	VI	VII	total	I	II	III	IV	V	VI	VII	total <sup>b</sup>
H-ZSM-5																
N <sub>2</sub> O (500 μl) <sup>c</sup>	–	1.3	–	–	–	–	–	1.3	–	–	–	–	–	–	1.3	–
NO (400 ppm) + C <sub>3</sub> H <sub>8</sub> (400 ppm)	–	–	–	4.2	0.6	1.4	–	6.2	–	–	–	0.7	0.1	0.6	–	1.4
NO (400 ppm)	–	–	–	4.6	4.5	2.3	–	11.4	–	–	–	0.7	0.8	0.5	–	2.0
NO (400 ppm) + O <sub>2</sub> (2.20 vol%)	–	–	–	–	–	–	1.3	1.3	–	–	–	–	–	–	–	–
Cu-ZSM-5																
N <sub>2</sub> O (500 μl) <sup>c</sup>	–	–	9.0	–	–	–	–	9.0	3.2	1.3	1.3	–	–	–	–	5.8
NO (400 ppm) + C <sub>3</sub> H <sub>8</sub> (400 ppm)	–	–	6.2	13.8	1.2	4.4	–	25.6	–	0.2	0.4	1.6	–	0.6	–	2.8
NO (400 ppm)	–	–	–	3.0	1.4	3.7	–	8.1	–	1.3	–	–	–	–	–	1.3
NO (400 ppm) + O <sub>2</sub> (2.20 vol%)	–	–	–	1.9	1.6	2.1	1.3	6.9	–	–	–	–	–	–	–	–
NO <sub>2</sub> (500 μl) <sup>d</sup>	–	–	–	0.5	1.6	2.2	1.3	5.6	–	–	–	–	–	–	–	–

<sup>a</sup>The data of table 4 were calculated based on separation of the N<sub>2</sub>O and N<sub>2</sub> TPD profiles on individual desorption peaks with computer processing of experimental profiles. The activation energies and pre-exponential factors of peaks are summarized in table 5. <sup>b</sup>The contribution of N<sub>2</sub> formed at nitrite–nitrate decomposition was subtracted from the total amount. <sup>c</sup>5 pulses of 100 μl of pure N<sub>2</sub>O were passed through the sample bed. <sup>d</sup>5 pulses of 100 μl of pure NO<sub>2</sub> were passed through the sample bed.

Table 5

Parameters<sup>a</sup> employed for the simulation of individual desorption peaks in the N<sub>2</sub>O and N<sub>2</sub> TPD over reduced Cu-ZSM-5 and reduced H-ZSM-5.

Gases adsorbed	Activation energy employed for the simulation of peaks (kcal mol <sup>-1</sup> )						
	peak I (100 °C)	peak II (135 °C)	peak III (160 °C)	peak IV (215 °C)	peak V (270 °C)	peak VI (320 °C)	peak VII (360 °C)
N <sub>2</sub> O (500 μl) <sup>b</sup>	14.7	16.5	18.1	–	–	–	–
NO (400 ppm) + C <sub>3</sub> H <sub>8</sub> (400 ppm)	–	16.5	18.1	20.7	23.3	26.0	–
NO (400 ppm)	–	–	–	20.8	23.3	26.0	–
NO (400 ppm) + O <sub>2</sub> (2.20 vol%)	–	–	–	20.5	23.5	26.0	27.8

<sup>a</sup>Pre-exponential factor equals  $1.0 \times 10^9 \text{ s}^{-1}$ , desorption order is 1 for all peaks. <sup>b</sup>5 pulses of 100 μl of pure N<sub>2</sub>O were passed through the sample bed.

the TPD profile of N<sub>2</sub> after the adsorption of N<sub>2</sub>O at the same temperature (figure 9(a)). The peak of N<sub>2</sub> at about 415 °C was ascribed to the decomposition of cis-nitrosyl–nitro complexes [24] formed after the adsorption of NO (figure 9(c)) as well as after the co-adsorption of NO and O<sub>2</sub> (figure 9(d)). The desorption of both N<sub>2</sub>O and N<sub>2</sub> significantly decreased over Cu-ZSM-5 in the presence of oxygen.

The fact that the amount of N<sub>2</sub>O desorbed at about 215 °C from the zeolite and especially from the catalyst depends on the C<sub>3</sub>H<sub>8</sub>/O<sub>2</sub> ratio in the adsorption mixture is a peculiarity of the system investigated. So, its amount gradually decreases in going from the NO + C<sub>3</sub>H<sub>8</sub> mixture to the NO<sub>2</sub> one (table 4, figure 8). It should be noted that maxima of the N<sub>2</sub>O desorption peaks coincide in both cases, i.e., they do not depend on the pretreatment procedure.

Summarizing this set of experiments, it is possible to conclude that the reduction of NO to N<sub>2</sub>O occurs on Cu ions and mainly on Fe impurities. The presence of copper as well as addition of oxygen appears to cause the oxidation of some iron cations from Fe<sup>2+</sup> to Fe<sup>3+</sup> leading to a decrease of the N<sub>2</sub>O formation. The N<sub>2</sub>O desorption peaks observed are a characteristic feature of the low-exchanged Cu-ZSM-5 catalysts.

## Acknowledgement

EVR would like to express his gratitude to the ISSEP for the financial support during this study (grants no. sn1480 and a96-1060). We also would like to thank O.V. Komova for preparation of the Cu-ZSM-5 sample.

## References

- [1] M. Iwamoto and H. Hamada, *Catal. Today* 10 (1991) 57.
- [2] J. Haggin, in: *C&EN* (8 January 1996).
- [3] R. Burch and P. Millington, *Appl. Catal. B* 2 (1993) 101.
- [4] B.J. Cho, *J. Catal.* 142 (1993) 418.
- [5] C.J. Bennet, P.S. Bennet, S.E. Golunski, J.W. Hayes and A.P. Walker, *Appl. Catal. A* 86 (1992) L1.
- [6] K.A. Bathke, C. Li, M.C. Kung, B. Yang and H.H. Kung, *Catal. Lett.* 31 (1995) 287.
- [7] H. Hamada, Y. Kintaichi, M. Sasaki, T. Ito and M. Tabata, *Appl. Catal.* 75 (1991) L1.
- [8] C.N. Montreuil and M. Shelef, *Appl. Catal. B* 1 (1992) L1.
- [9] B.J. Adelman, T. Beutel, G.-D. Lei and W.M.H. Sachtler, *Appl. Catal. B* 11 (1996) L1.
- [10] M. Iwamoto and H. Takeda, *Catal. Today* 27 (1996) 71.
- [11] F. Witzel, G.A. Sill and W.K. Hall, *J. Catal.* 149 (1994) 229.
- [12] Y. Li, T.L. Slager and J.N. Armor, *J. Catal.* 150 (1994) 229.
- [13] T. Beutel, B.J. Adelman, G.-D. Lei and W.M.H. Sachtler, *Catal. Lett.* 32 (1995) 83.

- [14] R.H.H. Smits and Y. Iwasawa, *Appl. Catal. B* 6 (1995) L201.
- [15] C. Yokoyama and M. Misono, *J. Catal.* 150 (1994) 9.
- [16] T. Beutel, B.J. Adelman and W.M.H. Sachtler, *Catal. Lett.* 37 (1996) 125.
- [17] D.J. Parrilo, *J. Catal.* 129 (1991) 202.
- [18] A. Sepulveda-Escribano, C. Marquez-Alvarez, I. Rodriguez-Ramos, A. Guerrero-Ruiz and J.L.G. Fierro, *Catal. Today* 17 (1993) 167.
- [19] A.V. Simakov, N.N. Sazonova, E.V. Rebrov, O.V. Komova and G.B. Barannik, in: *Proc. Russian-Korean Seminar on Catalysis*, Novosibirsk, 16–19 May 1995, p. 139.
- [20] V.V. Kharlamov, V.I. Bogomolov, N.V. Mirzabekova and A.V. Pospelov, *Zhurnal Fizicheskoi Khimii* 50 (1976) 343.
- [21] A.V. Simakov, *React. Kinet. Catal. Lett.* 97 (1996) 331.
- [22] S. Larsen, in: *Proc. US-Russia Workshop on Environ. Catal.*, Wilmington, DE, 1994, p. 21.
- [23] V.A. Sadykov, G.M. Alikina, R.V. Bunina, S.L. Baron, S.A. Veniaminov, V.N. Romannikov, V.P. Doronin, A.Ya. Rozovskii, V.F. Tretyakov, V.V. Lunin, E.V. Lunina, A.N. Kharlanov and A.V. Matyshak, in: *Proc. 1st World Congress Environ. Catal.*, Pisa, 1–5 May 1995, p. 315.
- [24] Y. Li and J.N. Armor, *Appl. Catal.* 76 (1991) L1.
- [25] Z. Chajar, M. Primet, H. Praliald, M. Chevrier, C. Gauthier and F. Mathis, *Catal. Lett.* 28 (1994) 33.
- [26] *CRC Handbook of Chemistry and Physics*, 73rd Ed. (CRC Press, Boca Raton, FL, 1992/1993) p. 121.
- [27] M. Iwamoto and H. Takeda, *Catal. Today* 27 (1996) 71.
- [28] N.N. Sazonova, O.V. Komova, E.V. Rebrov, A.V. Simakov, N.A. Kulikovskaya, V.A. Rogov, R.V. Olkhov and G.B. Barannik, *React. Kinet. Catal. Lett.* 60 (1997) 313.
- [29] Z. Schay and L. Guzzi, *Catal. Today* 17 (1993) 175.
- [30] M. Iwamoto, H. Yahiro, K. Tanda, N. Mizuno, Y. Mine and S. Kagawa, *J. Phys. Chem.* 95 (1991) 3727.
- [31] M. Sasaki, H. Hamada, Y. Kintaichi and T. Ito, *Catal. Lett.* 15 (1992) 297.
- [32] Y. Ukisu, S. Sato, A. Abe and K. Yoshida, *Appl. Catal. B* 2 (1993) 147.
- [33] K.A. Bethke, C. Li, M.C. Kung, B. Yang and H.H. Kung, *Catal. Lett.* 31 (1995) 287.
- [34] T. Beutel, J. Sarkany, G.-D. Lei, J.Y. Yan and W.M.H. Sachtler, *J. Phys. Chem.* 100 (1996) 845.
- [35] G.D. Lei, B.J. Adelman, J. Sarkany and W.M.H. Sachtler, *Appl. Catal. B* 5 (1995) 245.
- [36] J. Valyon and W.K. Hall, *J. Phys. Chem.* 97 (1993) 1204.
- [37] Z. Wang, A.V. Sklyarov and G.W. Keulks, *Catal. Today* 33 (1997) 291.
- [38] J. Valyon and W.K. Hall, *J. Catal.* 143 (1993) 520.
- [39] G. Spoto, S. Bordiga, D. Scarano and A. Zecchina, *Catal. Lett.* 13 (1992) 39.
- [40] Y. Li and W.K. Hall, *J. Catal.* 129 (1991) 202.
- [41] A.V. Kuchеров, G.L. Gerlock, H.-W. Jen and M. Shelef, *Catal. Today* 27 (1996) 79.
- [42] J. Leglise, J.O. Petunchi and W.K. Hall, *J. Catal.* 86 (1984) 392.
- [43] Y. Li and J.N. Armor, *Appl. Catal. B* 1 (1992) L21.